SQUARE-WAVE VOLTAMMETRY OF DECAMETHYLFERROCENE AT THE THREE-PHASE JUNCTION ORGANIC LIQUID/AQUEOUS SOLUTION/GRAPHITE

Šebojka KOMORSKY-LOVRIĆ[a,*], Milivoj LOVRIĆ[a] and Fritz SCHOLZ[b]

[a] *Center for Marine Research, "Ruder Bošković" Institute, POB 180, HR-10002 Zagreb, Croatia; e-mail: slovric@rudjer.irb.hr*

[b] *E.-M.-Arndt-Universität, Institut für Chemie, Soldtmannstrasse 23, 17489 Greifswald, Germany; e-mail: fscholz@rz.uni-greifswald.de*

Received October 16, 2000
Accepted December 5, 2000

Presented at the J. Heyrovský Memorial Symposium, Prague, August 30–September 1, 2000.

Drops of nitrobenzene and 1,2-dichloroethane with 0.1 M decamethylferrocene (dmfc) are attached to the surface of a paraffin-impregnated graphite electrode and immersed into various aqueous electrolytes. The oxidation of dmfc and the reduction of dmfc$^+$ cation are enabled by simultaneous transfers of anions between the aqueous electrolyte and the organic solvents. Square-wave voltammetry of this reaction is reported. A linear relationship was observed between the peak potentials of dmfc and the standard Galvani potential differences of the anions. The influence of the anion concentration on this relation is explained.

Keywords: Ion transfer; Square-wave voltammetry; Liquid/liquid interface; Nitrobenzene; Ferrocenes; Graphite electrode; Electrochemistry.

Electrode reactions of microparticles of some insoluble inorganic and organic solid compounds immobilized on the graphite and immersed in an electrolyte solution can be explained by coupled transfer of electrons and ions from the three-phase interface to the bulk of microparticle[1–6]. Electrons are exchange at the particle/graphite interface, while ions enter through the electrolyte/particle interface. Hence, the reaction starts at the junction of these two interfaces[7–9]. A well-defined three-phase boundary model was formed by attaching a droplet of nitrobenzene to the paraffin-impregnated graphite electrode (PIGE) immersed it into an aqueous electrolyte solution[10]. A decamethylferrocene (dmfc) was dissolved in nitrobenzene, but no supporting electrolyte was added to this solution. Upon anodic polarization of the PIGE, dmfc was oxidized in the nitrobenzene phase (nb) at the three-phase junction while simultaneously

doi: 10.1135/cccc20010434

anions of the aqueous electrolyte (w) were transferred across the water/nitrobenzene interface:

$$\mathrm{dmfc}_{\mathrm{nb}} + \mathrm{X}^{-}_{\mathrm{w}} \rightleftarrows \mathrm{dmfc}^{+}_{\mathrm{nb}} + \mathrm{X}^{-}_{\mathrm{nb}} + \mathrm{e}\ . \qquad (1)$$

The advantage of this experiment is the fact that the Gibbs energies of transfer of many cations and anions across the interface between two immiscible electrolyte solutions are known from independent studies[11–22]. Ion and electron transfers across the interface between immiscible electrolyte solutions and accompanying phenomena, such as the association of ions across the interface, specific adsorption at the interface and the formation of self-assembled monomolecular films, are studied extensively. These phenomena have an importance for determination of thermodynamic variables for solvent extractions and two-phase coupling reactions in the organic synthesis using the reverse phase-transfer catalysis, further for analysis of microscopic structure and dynamics of liquid/liquid interfaces, for the development of models of biological membranes, propagation of bioelectrochemical signals, cell respiration and photosynthesis[11,23–34]. Experiments with dmfc in nitrobenzene are partly related to this research area offering an access to the ion transfer energy data. It was demonstrated that the mid-potential of cyclic voltammograms depends linearly on the standard Galvani potential differences of transfer of anions between water and nitrobenzene. This was used to estimate the standard Gibbs energy of transfer of acetate and sulfate anions[35]. In this preliminary communication, application of the square-wave voltammetry to the electrode reaction at the three-phase boundary is reported.

EXPERIMENTAL

Decamethylferrocene (Fluka, Germany) was dissolved in nitrobenzene and 1,2-dichloroethane in a concentration of 0.1 mol l^{-1}. Aqueous electrolytes were prepared from analytical grade potassium and sodium salts. A drop of dmfc solution (2 μl) was attached to a paraffin-impregnated graphite electrode with an Eppendorf pipette. The drop covered about one half of the PIGE surface. The preparation of PIGE has been described previously[1]. Organic solvents were saturated with water and aqueous electrolytes were saturated with organic solvents. Deoxygenation of electrolyte solutions was achieved by purging with high-purity nitrogen for 20 min prior to experiments. A nitrogen protective atmosphere was maintained thereafter.

Square-wave voltammetry was performed by using a computer-controlled electrochemical measuring station Autolab (Eco-Chemie, Utrecht, Netherlands). A silver|silver chloride|3 M

KCl reference electrode (E = 0.208 V *vs* SHE) and a platinum wire auxiliary electrode was used.

RESULTS AND DISCUSSION

Square-wave voltammograms of dmfc in both nitrobenzene and 1,2-dichloroethane are well developed in the presence of all investigated anions of aqueous electrolytes. Typical examples are shown in Figs 1 and 2. The forward (oxidative) and the backward (reductive) components of the response are characteristic of reversible or quasi-reversible redox reactions[36]. In nitrobenzene, the ratio of the oxidation and reduction peak currents is 1.8 and the separation between the peak potentials of these components is 20 mV. The peak potentials of the net response are directly proportional to the standard Galvani potential differences of anions in aqueous electrolytes as shown in Fig. 3. The ion transfer potentials are compiled from the literature[12–15]. This result is in agreement with the relationship found in cyclic voltammetry[10]. It shows that the electrode reaction of dmfc in nitrobenzene is correctly interpreted by Eq. (*1*) and the cation dmfc$^+$ is not transferred into water under these experimental conditions. The latter conclusion is supported by the report of Zhang *et al.*[37]. If $D^{1/2}_{\mathrm{dmfc,nb}}[\mathrm{dmfc_{nb}}]^* = D^{1/2}_{\mathrm{X^-,w}}[\mathrm{X^-_w}]^*$, the reversible chronoamperometric half-wave potential of reaction (*1*) is independent of the concentrations of reagents[35]

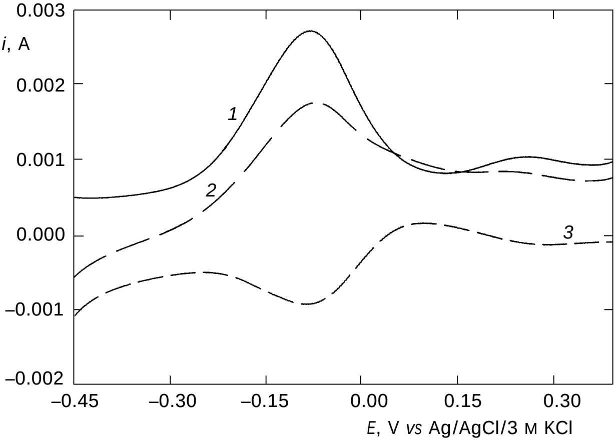

FIG. 1

Square-wave voltammogram of 0.1 M solution of dmfc in nitrobenzene immersed in aqueous 1 M KSCN. The net response (*1*) and its forward (*2*) and reverse (*3*) components. Square-wave frequency: 100 Hz

$$E_{1/2} = E^0_{\mathrm{dmfc/dmfc^+,nb}} + \Delta^{\mathrm{nb}}_{\mathrm{w}}\varphi^0_{\mathrm{X^-}} + \frac{RT}{F}\ln\frac{\gamma_{\mathrm{dmfc^+}}\gamma_{\mathrm{X^-_{nb}}}}{\gamma_{\mathrm{dmfc}}\gamma_{\mathrm{X^-_w}}} + \frac{RT}{F}\ln\frac{D^{1/2}_{\mathrm{dmfc}}D^{1/2}_{\mathrm{X^-_w}}}{D_1}\,. \qquad (2)$$

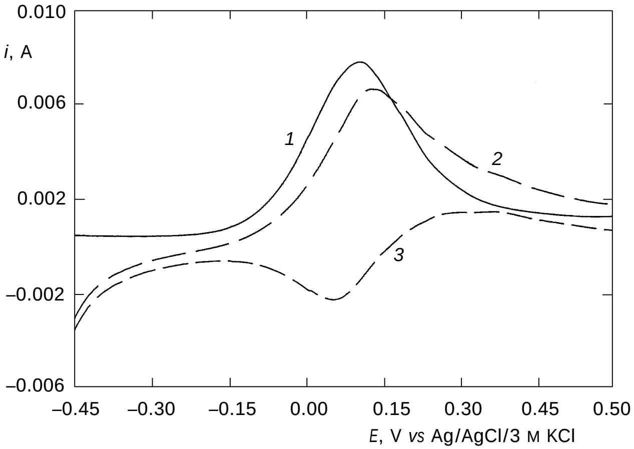

FIG. 2

Square-wave voltammogram of 0.1 M solution of dmfc in 1,2-dichloroethane immersed in aqueous 1 M KBr. The net response (*1*) and its forward (*2*) and reverse (*3*) components. Square wave frequency: 100 Hz

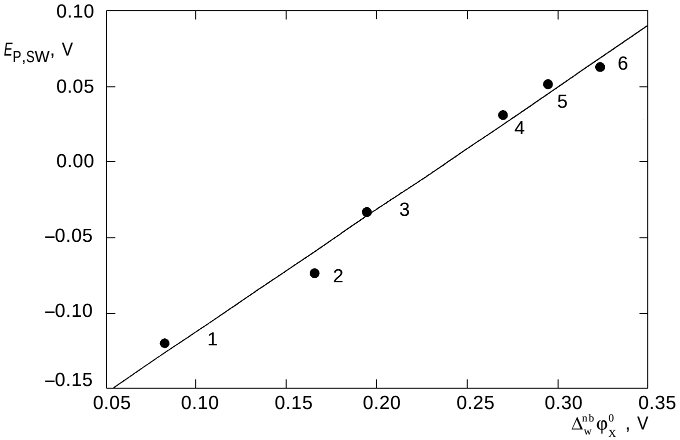

FIG. 3

The relationship between square-wave peak potentials of dmfc in nitrobenzene and the standard Galvani potential differences of anions in aqueous electrolytes: $\mathrm{ClO_4^-}$ (1), $\mathrm{SCN^-}$ (2), $\mathrm{I^-}$ (3), $\mathrm{NO_3^-}$ (4), $\mathrm{Br^-}$ (5) and $\mathrm{Cl^-}$ (6)

Here, D is the diffusion coefficient of dmfc, dmfc$^+$, X^-_{nb} and X^-_{w}, respectively (as indicated by index) $[\mathrm{dmfc_{nb}}]^*$ and $[X^-_{\mathrm{w}}]^*$ are bulk concentrations of dmfc in nitrobenzene and X$^-$ in the aqueous electrolyte, respectively, $E^0_{\mathrm{dmfc/dmfc^+}}$ is the standard potential of the redox couple dmfc/dmfc$^+$ in nitrobenzene, $\Delta^{\mathrm{nb}}_{\mathrm{w}}\varphi^0_{X^-}$ is the standard Galvani potential difference of the anion X$^-$ on the water/nitrobenzene interface and γ (as indicated by index) is the activity coefficient of dmfc$^+$, X^-_{nb}, dmfc and X^-_{w}, respectively. In nitrobenzene, the neutrality requires $\lfloor \mathrm{dmfc}^+_{\mathrm{nb}} \rfloor = \lfloor X^-_{\mathrm{nb}} \rfloor$ and therefore $D_{\mathrm{dmfc^+}} = D_{X^-_{\mathrm{nb}}} = D_1$. Besides, Zhang *et al.* have shown that $D_{\mathrm{dmfc^+}}/D_{\mathrm{dmfc}} = 0.85$ and $D_{\mathrm{dmfc}} = 7 \cdot 10^{-6}$ cm^2/s (ref.[37]). Previously, it was shown that the correlation of mid-peak potentials measured at lower scan rates with $\Delta^{\mathrm{nb}}_{\mathrm{w}}\varphi^0_{X^-}$ had the slope 0.9 ± 0.1 (refs[10,35]). The slope of the straight line in Fig. 3 is 0.85, which means that in nitrobenzene the square-wave peak potentials of dmfc are close to the reversible half-wave potentials.

The dependence of net square-wave peak-potentials of 0.1 M dmfc in nitrobenzene on the logarithm of aqueous electrolyte concentration is shown in Fig. 4. If the concentration of KNO_3 in water is higher than the concentration of dmfc in nitrobenzene, this relationship is linear, with the slope –0.052 V per decade of $[NO_3^-]$. If concentration of KNO_3 is lower than concentration of dmfc, the slope is 0.056 V per decade of $[NO_3^-]$. To explain these results, a simple mathematical model is developed in Appendix. Fig-

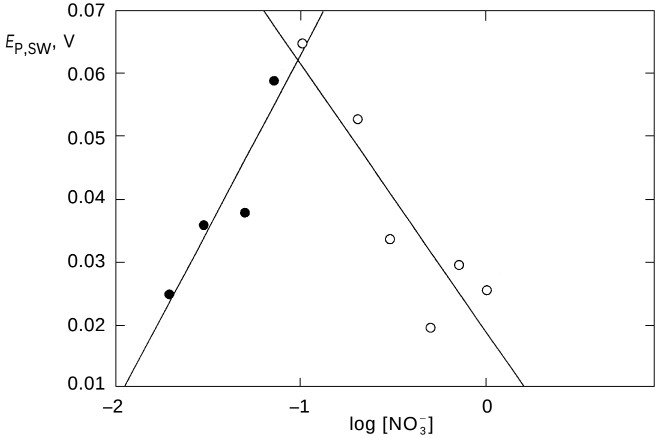

FIG. 4

Dependence of square-wave peak potentials of 0.1 M decamethylferrocene in nitrobenzene on the logarithm of concentration of aqueous KNO_3: ● diluted, ❍ concentrated electrolyte ure 5 shows theoretical square-wave voltammogram of the fast and reversible redox reaction (*1*). Its main characteristic is the dependence on the ratio $\rho = [X_w^-]^*/[\text{dmfc}]^*$, because it is the reaction of the second order. Dimensionless currents Φ are normalized to the bulk concentration of dmfc in organic solvent because usually $[\text{dmfc}]^* < [X_w^-]^*$. Generally, however, the current depends on bulk concentrations of both reactants. This can be seen in Fig. 6. Dimensionless peak currents are idependent of the ratio of bulk concentrations if $\rho \geq 10$. Under this condition real peak currents are directly proportional to [dmfc]* if increasing [dmfc]* does not change the ratio ρ below the limit given above. In the range of non-linear relationship between Φ_P and log ρ, real peak currents are linear functions of [dmfc]* only if the change of [dmfc]* is accompanied by a change in $[X_w^-]^*$, to maintain the constant ρ. Otherwise, the relation between real peak currents and [dmfc]* is not linear.

The ratio of dimensionless oxidation and reduction peak currents changes from 2.0 for ρ = 0.1 to 1.8 for ρ = 1 and 1.7 for $\rho \geq 10$. The separation between peak potentials of these components decreases from 20 mV for ρ = 1 to 10 mV for $\rho \geq 10$ and $\rho < 0.3$. According to these criteria, the square-wave response shown in Fig. 1 can be characterized as almost reversible.

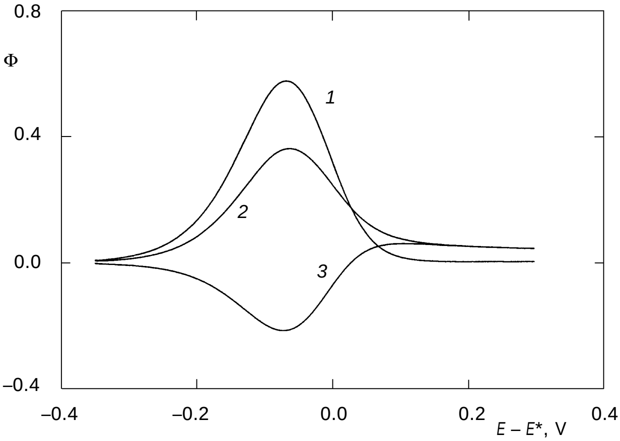

FIG. 5
Theoretical square-wave voltammogram of reversible redox reaction (Eq. (*1*)). The net response (*1*) and its forward (*2*) and reverse (*3*) components. Amplitude: 50 mV, d*E* = 2 mV, ρ = 10 and $\Phi = I(nFS\ [\text{dmfc}]^*)^{-1}(Df)^{-1/2}$

The theoretical dependence of peak potentials of the net response on the logarithm of the ratio ρ is shown in Fig. 7. If ρ ≥ 10, this relationship is linear with the slope $\partial E_{P,nett}/\partial \log \rho = -0.059$ V per decade of ρ, at 25 °C. If ρ = 1

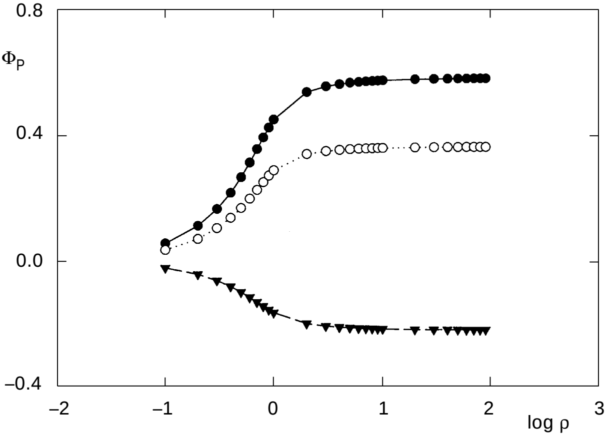

FIG. 6
The relationship between theoretical square-wave voltammetric peak currents and the logarithm of the ratio ρ. The net response (●) and its forward (❍) and reverse (▼) components

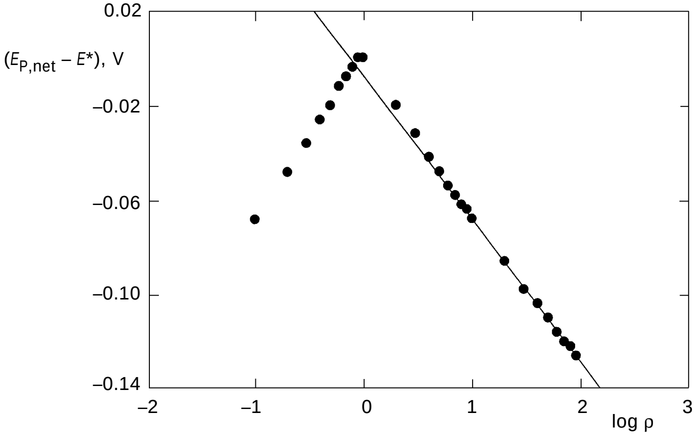

FIG. 7
The relationship between theoretical square-wave voltammetric peak potentials and the logarithm of the ratio ρ

and the difference between diffusion coefficients of dmfc and dmfc$^+$ cation is neglected, the net peak potential is

$$E_\mathrm{P} = E^0_{\mathrm{dmfc/dmfc^+,nb}} + \Delta_\mathrm{w}^\mathrm{nb}\varphi^0_{\mathrm{X^-}} + \frac{RT}{F}\ln\frac{\gamma_{\mathrm{dmfc^+}}\gamma_{\mathrm{X^-_{nb}}}}{\gamma_{\mathrm{dmfc}}\gamma_{\mathrm{X^-_w}}} \,. \tag{3}$$

In the range –1 < log ρ < 1, the relationships are not linear. If 0 < log ρ < 1, the average slope is –0.068 V per decade of ρ and if –1 < log ρ < 0, the average slope is 0.070 V per decade of ρ. Hence, if the concentration of aqueous electrolyte is much higher than the concentration of dmfc, the net peak potentials depend on the concentrations of both reactants

$$\begin{aligned} E_\mathrm{P} &= E^0_{\mathrm{dmfc/dmfc^+,nb}} + \Delta_\mathrm{w}^\mathrm{nb}\varphi^0_{\mathrm{X^-}} + \frac{RT}{F}\ln\frac{\gamma_{\mathrm{dmfc^+}}\gamma_{\mathrm{X^-_{nb}}}}{\gamma_{\mathrm{dmfc}}\gamma_{\mathrm{X^-_w}}} + \frac{RT}{F}\ln[\mathrm{dmfc}_\mathrm{nb}]^* - \\ &- \frac{RT}{F}\ln[\mathrm{X^-_w}]^* - \frac{RT}{2F}\ln 2 \,. \end{aligned} \tag{4}$$

This result is in agreement with the equations derived for cyclic voltammetry[10] and chronoamperometry[35]. It is also in qualitative agreement with experimental data shown in Fig. 4.

Under the influence of electrode and ion transfer kinetics, the reduction component of the theoretical square-wave response diminishes. An example is shown in Fig. 8. The ratio of the maximum oxidation current and the

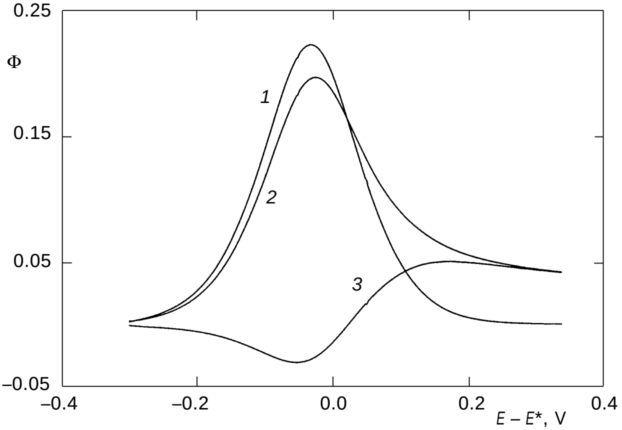

FIG. 8
Theoretical square-wave voltammogram of quasi-reversible redox reaction (Eq. (*1*)). The net response (*1*) and its forward (*2*) and reverse (*3*) components. Amplitude: 50 mV, dE = 2 mV, ρ = 10, α = 0.5 and k = 0.05

minimum reduction current is 6.7, while the separation between corresponding peak potentials is 30 mV. Both the ratio of peak currents and the peak separation increase with diminishing the rate constant, until the minimum of the backward component vanishes. The kinetic parameters were varied in order to simulate the response shown in Fig. 2. The peak currents ratio in this figure is 2.8, but the separation of peaks is as high as 76 mV. This indicates that the square-wave voltammetric response of dmfc in dichloroethane is kinetically controlled, but the mechanism of this reaction cannot be explained by a simple model developed in this paper.

It can be concluded that square-wave voltammetry can provide information about the kinetics of ion transfer across the water/organic solvent interface.

APPENDIX

In the case of local equilibrium at the three-phase junction (x = 0), the redox reaction (*1*) is defined by the Nernst equation

$$E = E^0_{\mathrm{dmfc/dmfc^+}} + \Delta^{\mathrm{nb}}_{\mathrm{w}}\varphi^0_{\mathrm{X^-}} + \frac{RT}{F}\ln\left(\frac{a_{\mathrm{dmfc^+}}a_{\mathrm{X^-_{nb}}}}{a_{\mathrm{dmfc}}a_{\mathrm{X^-_w}}}\right)_{x=0} - \Delta\varphi_{\mathrm{lj}} + I(R_{\mathrm{nb}} + R_{\mathrm{w}})\ , \qquad (A1)$$

where E is the electrode potential, $(a_{\mathrm{dmfc,nb}})_{x=0}$ and $(a_{\mathrm{dmfc^+,nb}})_{x=0}$ are the activities of dmfc and dmfc$^+$ in nitrobenzene at the three-phase junction, respectively, $(a_{\mathrm{X^-_{nb}}})_{x=0}$ and $(a_{\mathrm{X^-_w}})_{x=0}$ are the activities of the anion X$^-$ in nitrobenzene and water, respectively, both at the three-phase junction, $\Delta\varphi_{\mathrm{ij}}$ is the liquid junction potential between the aqueous electrolyte and the reference electrode, I is current and R_{nb} and R_{w} are the resistances of nitrobenzene and the aqueous electrolyte, respectively. The meanings of other symbols were already explained. Assuming that the planar diffusion model can be used as a first approximation of the transport and that differences between diffusion coefficients can be neglected, the concentrations of reactants and products at the three-phase bounadry are given by integral equations

$$[\mathrm{dmfc}]_{x=0}/[\mathrm{dmfc}]^* = 1 - (f/\pi)^{1/2}\int_0^t \Phi(t-\tau)^{-1/2}\,\mathrm{d}\tau\ , \qquad (A2)$$

$$[\mathrm{X^-_w}]_{x=0}/[\mathrm{dmfc}]^* = \rho - (f/\pi)^{1/2}\int_0^t \Phi(t-\tau)^{-1/2}\,\mathrm{d}\tau\ , \qquad (A3)$$

$$[\mathrm{dmfc}^+]_{x=0}/[\mathrm{dmfc}]^* = (f/\pi)^{1/2}\int_0^t \Phi(t-\tau)^{-1/2}\,\mathrm{d}\tau\,, \qquad (A4)$$

where $\Phi = I(nFS\,[\mathrm{dmfc}]^*)^{-1}(Df)^{-1/2}$, $\rho = [\mathrm{X}_\mathrm{w}^-]^*/[\mathrm{dmfc}]^*$, f is the square-wave frequency and S is a hypothetical active area of the three-phase junction. The assumption of planar transport is partly justified in the report of Myland and Oldham who demonstrated that the model based on cylindrical diffusion does not match experimental results[38] .They proposed that the active area of the drop is a narrow zone in the vicinity of the three-phase boundary.

The influence of electrode and ion transfer kinetics is simulated by the Butler–Volmer equation

$$\Phi = -k\exp(-\alpha\varphi)\left([\mathrm{dmfc}^+]^2_{x=0} - \exp(\varphi)[\mathrm{dmfc}]_{x=0}[\mathrm{X}_\mathrm{w}^-]_{x=0}\right)([\mathrm{dmfc}]^*)^{-2}\,, \qquad (A5)$$

where $\varphi = F(E - E_\mathrm{f})/RT$ is a dimensionless potential, $k = k_\mathrm{s}[\mathrm{dmfc}]^*(Df)^{-1/2}$ is a dimensionless rate constant, k_s is a standard rate constant, α is a transfer coefficient and

$$E_f = E^0_{\mathrm{dmfc/dmfc^+,nb}} + \Delta^{\mathrm{nb}}_{\mathrm{w}}\varphi^0_{\mathrm{X}^-} + \frac{RT}{F}\ln\frac{\gamma_{\mathrm{dmfc}^+}\gamma_{\mathrm{X}^-_{\mathrm{nb}}}}{\gamma_{\mathrm{dmfc}}\gamma_{\mathrm{X}^-_{\mathrm{w}}}}\,.$$

The kinetics of interfacial ion transfer was interpreted by several mechanisms[11], but the Butler–Volmer equation is still widely used[39].

Integral equations (*A1*)–(*A5*) were solved by numerical integration method described previously[40]. The time increment was $d = (50f)^{-1}$.

The authors acknowledge support of Fonds der Chemischen Industrie and of the respective ministries in the framework of a bilateral German–Croatian Scientific Research Program.

REFERENCES

1. Scholz F., Meyer B. in: *Voltammetry of Solid Microparticles Immobilized on Electrode Surfaces*, in *Electroanal. Chem.* (A. J. Bard and I. Rubinstein, Eds), Vol. 20, p. 1. Marcel Dekker, New York 1998.
2. Komorsky-Lovrić Š.: *J. Solid State Electrochem.* **1997**, *1*, 94.
3. Schröder U., Scholz F.: *J. Solid State Electrochem.* **1997**, *1*, 62.
4. Dostál A., Hermes M., Scholz F.: *J. Electroanal. Chem.* **1996**, *415*, 133.
5. Bond A. M., Marken F.: *J. Electroanal. Chem.* **1994**, *372*, 125.

6. Komorsky-Lovrić Š., Mirčeski V., Scholz F.: *Mikrochim. Acta* **1999**, *132*, 67.
7. Lovrić M., Scholz F.: *J. Solid State Electrochem.* **1999**, *3*, 172.
8. Maser K.: *J. Solid State Electrochem.* **1999**, *4*, 3.
9. Schröder U., Oldham K. B., Myland J. C., Mahon J. P., Scholz F.: *J. Solid State Electrochem.* **2000**, *4*, 314.
10. Scholz F., Komorsky-Lovrić Š., Lovrić M.: *Electrochem. Commun.* **2000**, *2*, 112.
11. Girault H. H. J., Schiffrin D. J.: *Electrochemistry of Liquid–Liquid Interfaces*, in *Electroanal. Chem.* (A. J. Bard, Ed.), Vol. 15, p. 1. Marcel Dekker, New York 1989.
12. Rais J.: *Collect. Czech. Chem. Commun.* **1971**, *36*, 3256.
13. Rais J., Selucky P., Kyrs M.: *J. Inorg. Nucl. Chem.* **1976**, *38*, 1376.
14. Hundhammer B., Solomon T.: *J. Electroanal. Chem.* **1983**, *157*, 213.
15. Hundhammer B., Wilke S.: *J. Electroanal. Chem.* **1989**, *266*, 133.
16. Osakai T., Ogata A., Ebina K.: *J. Phys. Chem. B* **1997**, *101*, 8341.
17. Czapkiewicz J., Czapkiewicz-Tutaj B.: *J. Chem. Soc., Faraday Trans. 1* **1980**, *76*, 1663.
18. Sabela A., Mareček V., Samec Z., Fuoco R.: *Electrochim. Acta* **1992**, *37*, 231.
19. Mickler W., Mönner A., Uhlemann E., Wilke S., Müller H.: *J. Electroanal. Chem.* **1999**, *469*, 91.
20. Kong Y.-T., Kakiuchi T.: *J. Electroanal. Chem.* **2000**, *483*, 22.
21. Rais J., Okada T.: *J. Phys. Chem. A* **2000**, *104*, 7314.
22. Katano H., Kuboyama H., Senda M.: *J. Electroanal. Chem.* **2000**, *483*, 117.
23. Amemiya S., Ding Z., Zhou J., Bard A. J.: *J. Electroanal. Chem.* **2000**, *483*, 7.
24. Lu Z., Sun Z., Dong S.: *Electroanalysis (N. Y.)* **1989**, *1*, 271.
25. Strutwolf J., Barker A. L., Gonsalves M., Caruana D. J., Unwin P. R., Williams D. E., Webster J. R. P.: *J. Electroanal. Chem.* **2000**, *483*, 163.
26. Shao Y., Mirkin M. V.: *Anal. Chem.* **1998**, *70*, 3155.
27. Mareček V., Lhotsky A., Jänchenova H.: *J. Electroanal. Chem.* **2000**, *483*, 174.
28. Pecina O., Badiali J. P.: *J. Electroanal. Chem.* **1999**, *475*, 46.
29. Allen R. M., Kontturi K., Murtomäki L., Williams D. E.: *J. Electroanal. Chem.* **2000**, *483*, 57.
30. Lahtinen R., Fermin D. J., Kontturi K., Girault H. H.: *J. Electroanal. Chem.* **2000**, *483*, 81.
31. Baars A., Aoki K., Watanabe J.: *J. Electroanal. Chem.* **1999**, *464*, 128.
32. Ohde H., Maeda K., Yoshida Y., Kihara S.: *J. Electroanal. Chem.* **2000**, *483*, 108.
33. Josserand J., Morandini J., Lee H. J., Ferrigno R., Girault H. H.: *J. Electroanal. Chem.* **1999**, *468*, 42.
34. Volkov A. G.: *J. Electroanal. Chem.* **2000**, *483*, 150.
35. Komorsky-Lovrić Š., Lovrić M., Scholz F.: *J. Electroanal. Chem.*, submitted.
36. O'Dea J. J., Osteryoung J., Osteryoung R. A.: *Anal. Chem.* **1981**, *53*, 695.
37. Zhang J., Barker A. L., Unwin P. R.: *J. Electroanal. Chem.* **2000**, *483*, 95.
38. Myland J. C., Oldham K. B.: *Electrochem. Commun.* **2000**, *2*, 541.
39. Manzanares J. A., Allen R. M., Kontturi K.: *J. Electroanal. Chem.* **2000**, *483*, 188.
40. Lovrić M.: *Elektrokhimiya* **1996**, *32*, 1068.